Article

Not peer-reviewed version

Hydrogels Poly(vinyl alcohol)/Gentamicin and Poly(vinyl alcohol)/Chitosan/Gentamicin: A Promising Approach to Accelerate Burn Wound Healing

Anja Nikolić , Ivan Milošević * , Ana Janković * , Bogomir Bolka Prokić , Emilija Nićković , Danica Marković , Milena Stevanović , Maja Vukašinović-Sekulić , Vesna Mišković-Stanković , Tijana Lužajić Božinovski

Posted Date: 7 April 2025

doi: 10.20944/preprints202504.0504.v1

Keywords: in vitro; in vivo; wound dressing; rat; regeneration; skin

 doi:10.20944/preprints202504.0504.v1

Article

Hydrogels Poly(vinyl alcohol)/Gentamicin and Poly(vinyl alcohol)/Chitosan/Gentamicin: A Promising Approach to Accelerate Burn Wound Healing

Anja Nikolić [1], Ivan Milošević [1]*, Ana Janković [2]*, Bogomir B Prokić [3], Emilija Nićković [1], Danica Marković [1], Milena Stevanović [2], Maja Vukašinović-Sekulić [4], Vesna Mišković-Stanković [5] and Tijana Lužajić Božinovski [1]

[1] Department of Histology and Embryology, Faculty of Veterinary Medicine, University of Belgrade, Bulevar oslobodjenja 18, 11000 Belgrade, Serbia. A.N. anja.nikolic@vet.bg.ac.rs; I.M. ikavet@vet.bg.ac.rs; E.M. nickovic.emilija@gmail.com; D.M. danica@vet.bg.ac.rs; T.L.B. ticavet@vet.bg.ac.rs

[2] Innovation Center of the Faculty of Technology and Metallurgy, University of Belgrade, Karnegijeva 4, 11000 Belgrade, Serbia. A.J. ajankovic@tmf.bg.ac.rs; M.S. mstevanovic@tmf.bg.ac.rs

[3] Department of Surgery, Orthopedy and Ophthalmology, Faculty of Veterinary Medicine, University of Belgrade, Bulevar oslobodjenja 18, 11000 Belgrade, Serbia. bbprokic@gmail.com

[4] Department of Biochemical Engineering and Biotechnology, Faculty of Technology and Metallurgy, University of Belgrade, Karnegijeva 4, 11000 Belgrade, Serbia. vukasinovic@tmf.bg.ac.rs

[5] Faculty of Ecology and Environmental Protection, University Union - Nikola Tesla, Cara Dušana, 11000 Belgrade, Serbia. vesna.miskovicstankovic@unionnikolatesla.edu.rs

* Correspondence: I.M. ikavet@vet.bg.ac.rs; A.J. ajankovic@tmf.bg.ac.rs

Abstract: Scar formation and delayed wound healing pose significant challenges in treating skin injuries, especially in severe cases like burns and diabetic wounds. This study investigates the effectiveness of novel Poly(vinyl alcohol) (PVA) / Gentamicin (Gent) and PVA / Chitosan (CHI) / Gent hydrogels in promoting healing of second-degree burn wounds in a rat model. Following *in vitro* testing, these hydrogels were deemed non-toxic and suitable for *in vivo* analysis. Clinical evaluations were conducted on 3rd, 7th, 14th and 21st post-injury day, assessing parameters such as blistering, edema, redness, crust, bleeding, secretion, scar tissue formation, and wound contraction percentage. Histological analyses focused on re-epithelization and dermal evaluation at specific time points. Results showed that both hydrogels significantly reduced inflammation, particularly redness, by the 14th day, and improved re-epithelization, with the PVA/CHI/Gent group outperforming on the 14th day and the PVA/Gent group excelling at the 21st day. Histological findings indicated increased fibroblast proliferation and collagen deposition in treated groups, suggesting enhanced dermal healing. The PVA/CHI/Gent hydrogel demonstrated notable antibacterial properties, likely due to the synergistic effects of CHI and Gent, leading to reduced inflammation and edema. Overall, both hydrogels show promise as effective wound dressings, facilitating faster healing and improved tissue recovery in burn injuries. This study supports the use of biomimetic scaffolds for enhanced wound management in clinical practices.

Keywords: *in vitro*; *in vivo*; wound dressing; rat; regeneration; skin

1. Introduction

Scar formation and delayed wound healing are significant challenges in treating skin tissue trauma [1,2]. Wound healing and tissue regeneration are a dynamic physiological process influenced by the interactions of the extracellular matrix, various cell types, and growth factors [3]. In severe conditions like trauma, diabetic or burn wounds, the normal processes of re-epithelialization and

 doi:10.20944/preprints202504.0504.v1

dermal repair may be insufficient for healing ([4]. Debridement, pressure reduction, and infection prevention are traditional wound treatment methods [5]. While effective for most injuries, larger skin wounds may need dressings that mimic skin tissue to support cell adhesion, migration, proliferation, and tissue generation by mimicking the extracellular matrix (ECM) [6]. Recent advancements in biomimetic scaffolds utilizing stem cells and bioactive substrates have created promising therapeutic options for treating full-thickness skin injuries [7]. Various materials and structures, such as hydrogels, films, and foams, are used as scaffolds to enhance healing and protect the skin from additional damage, because they possess ECM-like structure, high porosity, and permeability [6]. Hydrogels are regarded for ideal skin substitutes due to their moisture retention, effective fluid absorbance, and high water retention capacity [8,9]. Their porous structure provides support in absorbing wound exudate, minimizing infection risk, and promoting an environment conducive to wound healing [8,9]. Additionally, utilization of natural-synthetic polymer composites in hydrogel fabrication results in a porous structure that benefit from the biocompatibility of natural polymers and the customizable properties of synthetic polymers [10].

Poly(vinyl alcohol) (PVA) is a synthetic polymer widely used in tissue engineering due to its excellent biocompatibility, biodegradability, non-toxicity, non-carcinogenicity, and water solubility [11]. This cost-effective polymer possesses favorable physical properties, including good transparency, low interfacial tension, and a high swelling ratio. To improve mechanical properties, PVA has often been combined with natural polymers, as is PVA/chitosan composite hydrogel, with enhances softness and flexibility [10,12].

Chitosan (CHI), a polysaccharide-based polymer, is particularly effective in wound healing due to its ability to reduce pain by blocking nerve endings [12]. It accelerates natural blood clot formation and minimizes scarring [13]. Chitosan-based hydrogels possess excellent bioadhesive properties, prevent microbial penetration, control inflammation, and enhance natural hyaluronic acid levels at the wound site [14]. Structurally similar to glycosaminoglycans in the ECM, CHI boosts fibroblast activation, regulates collagen fiber density and distribution, and promotes cell migration, granulation tissue formation, and vascularization - essential processes in wound healing [13]. Its stimulating effect on leukocytes and potent antibacterial properties make CHI a widely used biomaterial in wound care [14].

Gentamicin (Gent) is an aminoglycoside antibiotic known for its effective antimicrobial activity, making it widely used in treating microbial infections, particularly burn wounds [15]. However, its ability to penetrate the deeper layers of skin is limited due to low systemic absorption, likely because of its cationic nature [16,17]. Consequently, Gent primarily exerts its effects on the superficial skin layer. Despite its efficacy, Gent can cause renal tubular necrosis and congestion [18], as well as harm intra-auricular lymphocytes, leading to nephrotoxicity and ototoxicity, which somewhat restricts its clinical use [19]. To mitigate these toxic effects, researchers have explored methods to control Gent release by embedding or fixing it, allowing for sustained action [20]. Alternatively, Gent can be delivered directly to the target site for specific binding, enhancing its prolonged effect [21].

The aim of this study was to synthesize PVA/Gent and PVA/CHI/Gent hydrogels, and conduct an *in vivo* experiment using a rat model to investigate the potential promoting effect of the PVA/Gent and PVA/CHI/Gent hydrogels on burn wound healing. These innovative hydrogels, originally synthesis in our laboratory and applied for the first time in *in vivo* experiments, should enable the long-term controlled release of embedded Gent in the wound locally, avoiding the systemic antibiotic administration.

2. Results and Discussion

2.1. Antibacterial Activity

Prior to the conducting of the *in vivo* experiment antibacterial activity of synthesized hydrogels with different combinations of substances (PVA, CHI and Gent) were examined.

 doi:10.20944/preprints202504.0504.v1

Figure 1 represents photographs of disc-diffusion tests against *E. coli* and *S. aureus* of PVA, PVA/Gent, PVA/CHI and PVA/CHI/Gent hydrogels.

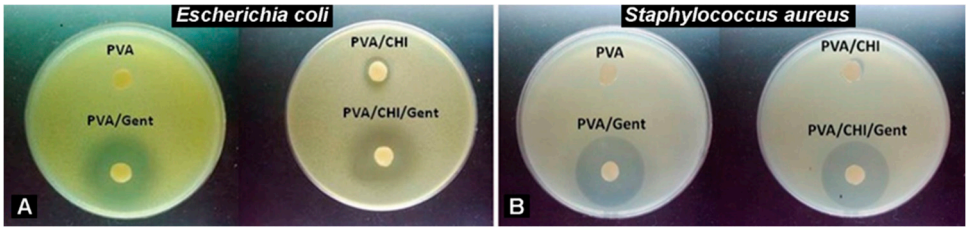

Figure 1. (A) Disc-diffusion test for *E. coli*; (B) *S. aureus* in the presence of hydrogels.

Hydrogel comprised of PVA did not exhibit any antibacterial effect on the tested bacterial strains. Evidently, all the samples with CHI showed certain antibacterial activity, which was stronger against *E. coli* than *S. aureus*. The average width of the inhibition zone against *S. aureus* was 12 mm. In the case of *E. coli*, two distinct regions of sensitivity are observed; highly sensitive zone of 12 mm and the moderate sensitivity zone of 14 mm in diameter. As expected, the zones of inhibition are clearly visible for all Gent containing hydrogels. Hydrogel PVA/Gent had a pronounced highly sensitive zone of 24.5 mm and the moderate sensitivity zone of 34 mm in diameter when tested against *E. coli*. The same sample acted very efficiently against *S. aureus*, since the inhibition zone was 31.5 mm in diameter. In the case of PVA/CHI/Gent, the addition of antibiotic increased the antibacterial activity of hydrogels. Against *S. aureus* PVA/CHI/Gent gave 31 mm wide zone of inhibition. When tested against *E. coli* difference in bacterial sensitivity was observed with a lighter colored, highly sensitive zone of 31 mm and the darker colored, moderate sensitivity zone of 33 mm in diameter (Figure 1 A, B).

The results obtained by disc-diffusion test are in accordance with the kinetics of antibacterial activity against *E. coli* ATCC25922 and *S. aureus* [22]. In the case of Gram-negative *E. coli*, PVA/Gent and PVA/CHI/Gent hydrogels exhibited a bactericidal effect, since the reduction of the number of viable bacterial colonies was more than three orders of magnitude after only 15 min of incubation. After 1h of inoculation, a sterile environment was achieved since there were no longer any live *E. coli* cells present. For the Gram-positive *S. aureus*, the absence of any live cells was observed after only 15 min. The mechanisms of antibacterial activity can be explained as follows. Gentamicin exerts its antibacterial effect by irreversibly binding to the 30S ribosomal subunit and 16S rRNA in bacterial cells. This interaction disrupts tRNA recognition, leading to misreading of mRNA and preventing the synthesis of essential proteins. Specifically, Gent binds to four nucleotides of 16S rRNA and an amino acid in the S12 protein, interfering with the ribosomal decoding site. As a result, incorrect amino acids are incorporated into the growing polypeptide chain, ultimately disrupting protein function and bacterial survival [23].

2.2. Gentamicin Release

To investigate the kinetics and mechanism of Gent release from PVA/Gent and PVA/CHI/Gent hydrogels, the experimental releasing profile of Gent has been determined using HPLC techniques, as the time dependence of the ratio c_t/c_o, where c_t is the concentration of Gent released from hydrogel at time, t and c_o is the initial concentration of Gent inside the hydrogel [22]. The experimental data were compared to several theoretical models in order to elucidate the Gent diffusion coefficient. The models applied were Makoid-Banakar [24], Korsmeyer-Peppas [25] and Kopcha [26] described by equations Eqs. (1), (2) and (3), respectively:

$$\frac{C_t}{C_0} = k_{MB} \cdot t^n \cdot \exp(-c \cdot t) \quad (1)$$

$$\frac{C_t}{C_0} = k_{KP} \cdot t^n \quad (2)$$

 doi:10.20944/preprints202504.0504.v1

$$\frac{c_t}{c_0} = A \cdot t^{1/2} + B \cdot t \quad (3)$$

where k_{MB} is the Makoid-Banakar constant; c is the Makoid-Banakar parameter; k_{KP} is the Korsmeyer-Peppas constant; n - the coefficient which describes release transport mechanism (n<0.5 - Fickian diffusion, n>0.5 - non-Fickian/anomalous diffusion, n=1 - Case II transport) [25]; A and B - Kopcha's constants which depend on the dominant transport phenomenon during release.

Gentamicin release profiles verified the initial burst release effect of Gent from the hydrogel, i.e., 70% loaded antibiotic was released within the first 48h which could be very useful in preventing biofilm formation, followed by slow release of Gent in a later time period. The time exponent, n, is an indication of the dominant diffusion mechanism and, as its values were less than 0.5, it can be concluded that the release of Gent from hydrogel conformed to the Fickian diffusion behavior [25] and was governed mainly by the concentration gradient of released Gent. This was also proved by Kopcha model, as the absolute values of parameter A were higher compared to B, indicating that the predominant driving force for the release is the diffusion, and not the polymer matrix relaxation.

In order to determine the value of diffusion coefficient of Gent, the early time approximation (ETA) model was applied and compared to diffusion coefficient calculated from GFD model. For ETA, two equations were used, standard ETA Eqs. (4) and a modified ETA Eqs. (5) proposed by Ritger and Peppas [27]. According to Ritger and Peppas, the standard ETA is frequently misused, even though it only applies to very specific cases of swelling, and for specific geometries of thin films with very high aspect ratio (diameter divided by thickness; a thin film will typically have aspect ratio of the order of ~100, whereas for thick hydrogel discs it is closer to unity) [27]. In these equations, c_t/c_0 denotes the fraction of released Gent at the time t, D is the diffusion coefficient of Gent during the release, t is the time of release, δ is the hydrogel thickness and r is the radius of the hydrogel disc:

$$\frac{c_t}{c_0} = 4 \cdot \left(\frac{D \cdot t}{\pi \cdot \delta^2}\right)^{1/2} \quad (4)$$

$$\frac{c_t}{c_0} = 4 \cdot \left(\frac{D \cdot t}{\pi \cdot r^2}\right)^{1/2} - \pi \cdot \left(\frac{D \cdot t}{\pi \cdot r^2}\right) - \frac{\pi}{3} \cdot \left(\frac{D \cdot t}{\pi \cdot r^2}\right)^{3/2} + 4 \cdot \left(\frac{D \cdot t}{\pi \cdot \delta^2}\right)^{1/2} \quad (5)$$

$$- \frac{2r}{\delta} \cdot \left[8 \cdot \left(\frac{D \cdot t}{\pi \cdot r^2}\right) - 2\pi \cdot \left(\frac{D \cdot t}{\pi \cdot r^2}\right)^{3/2} - \frac{2\pi}{3} \cdot \left(\frac{D \cdot t}{\pi \cdot r^2}\right)^2\right] \quad (6)$$

The ETA models represent the dependence of the fraction of released Gent on the square root of the release time while diffusion coefficient (D) of Gent release was determined from the slope of initial linear part of the experimental curve. Using modified ETA model, the values of D was calculated to be 7.16 x10^{-8} $cm^2\ s^{-1}$ for PVA/Gent hydrogel and 4.29x10^{-8} $cm^2\ s^{-1}$ for PVA/CHI hydrogel, meaning that the release of Gent is slower from the hydrogel with CHI due to greater number of bonds and consequently more crosslinked polymer matrix [28].

2.3. In Vivo Testing

The PVA/Gent and PVA/CHI/Gent hydrogels have been characterized, based on the material cytotoxicity scale [29], as non-toxic and suitable for *in vivo* testing [22]. Tests conducted on MTT assays even showed that PVA/CHI/Gent samples promote differentiation and growth of MRC-5 (human fibroblasts), as evidenced by cell viability value higher than 100%. However, in the case of L929 cells, the viability was slightly decreased for all samples, which could be due to the enhanced sensitivity of the mice cell line toward our samples. These results are promising, as the main concern with biomaterials revolves around their immediate application and potential impact on surrounding tissue.

The *in vivo* analysis aimed to capture all phases of wound repair - inflammation, proliferation, and remodeling - by analyzing the wounds on the 3rd, 7th, 14th, and 21st day post-injury [30]. Inflammation begins with vascular responses and neutrophil infiltration, later transitioning to macrophage dominance, leading to the proliferative phase, which involves the formation of

 doi:10.20944/preprints202504.0504.v1

epithelium and granulation tissue, consisting of fibroblasts, collagen, and new blood vessels [31]. Semi-quantitative scales were used to assess healing parameters, reflecting standard practices in the literature [32-35].

2.4. Clinical evaluations of the burn wound and wound contraction

Throughout evaluation of PVA/Gent and PVA/CHI/Gent wound healing efficacy on second-degree burns in Wistar rats, the tested hydrogels demonstrated good handling properties and hydrophilicity, allowing easy adherence to the wound bed. During the dressing changes for measurement and photography, the newly formed tissue remained intact, and the hydrogels did not adhere to the wound.

Both hydrogels demonstrated enhanced healing relative to the Ctr group, showing reductions in all clinical parameters (blistering, edema, redness, crust, bleeding, secretion, and scar tissue), notably a significant decrease in redness by day 14th ($p<0.05$) (Figure 2 A, B, C, D). Considering that redness (*rubor*) was defined as one of cardinal signs of inflammation 2000 years ago [36], its reduction confirms that both hydrogels reduce inflammation which is also in accordance with pronounced antibacterial activity of hydrogels containing Gent shown in the 2.1. section.

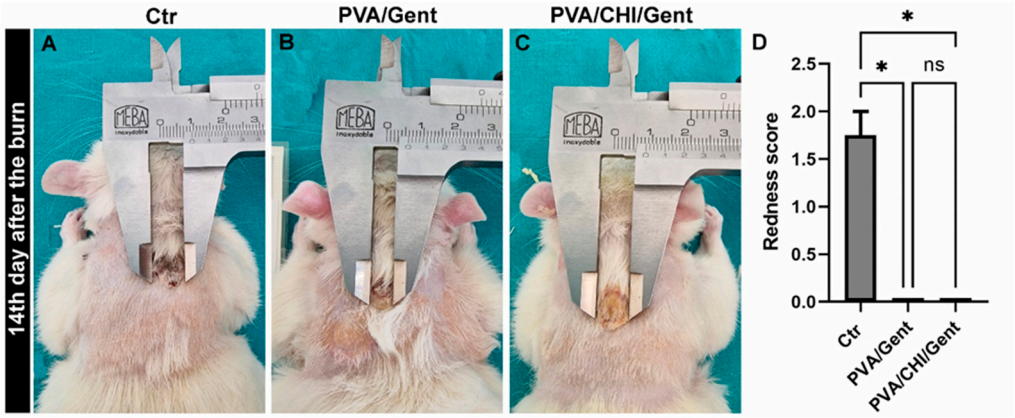

Figure 2. Representative photographs of burn wounds at the 14th day period from the (**A**) Control (Ctr); (**B**) Poly(vinyl alcohol) / Gentamicin (PVA/Gent) treated group; (**C**) Poly(vinyl alcohol) / Chitosan / Gentamicin (PVA/CHI/Gent) treated group; (**D**) boxplot showcasing redness scores compared by Kruskal-Wallis test + Dunn's test. Boxes indicate the lower to upper quartile (25th-75th percentile) and median value. Whiskers extend to minimum and maximum values. Statistical significance is denoted as *$p<0.05$.

Wound contraction, a key indicator of healing, was monitored, as an important part of the healing process of full-thickness wounds both in humans and in rats [12]. By the 3rd day period, the wound area slightly increased in both the Ctr and PVA/Gent groups compared to the initial measurement, while it decreased to a certain extent in the PVA/CHI/Gent treated group potentially due to CHI's ability to stimulate angiogenesis and fibroblast growth [37,38]. The property of CHI to unable the extension of burn wound in the period of three days post induction is described in literature [39]. Throughout all other time periods, a reduction in wound area compared to the initial measurements was observed in all groups. While no significant differences were observed among groups by the study's end, both PVA/Gent and PVA/CHI/Gent groups consistently exhibited smaller wound areas than the Ctr group, indicating that both hydrogels promote wound repair. This was most pronounced on the 14th day, with the Ctr group's wound area measuring 64.47 ± 26.51 mm^2, compared to 45.55 ± 17.33 mm^2 in the PVA/Gent group and 47.41 ± 11.03 mm^2 in the PVA/CHI/Gent treated group (Figure 3).

 doi:10.20944/preprints202504.0504.v1

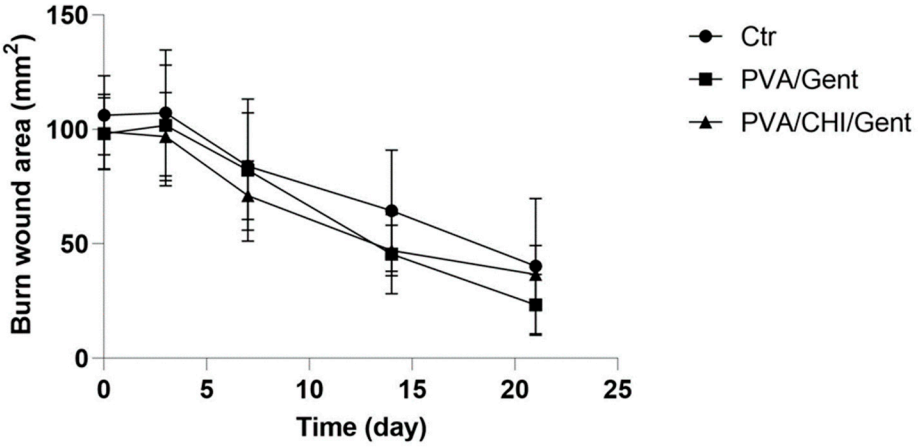

Figure 3. The graph depicting the wound area over time in the Ctr (line with circle), PVA/Gent treated (line with square) and PVA/CHI/Gent treated group (line with triangle).

2.5. Histological Analysis

The histological analysis showed that the effects of PVA/Gent and PVA/CHI/Gent hydrogels on re-epithelization and healing processes in the dermis were not uniform and were significant in different time periods.

Both hydrogels caused improvement of the re-epithelization process, which is depicted by representative microphotographs and graphs in Figure 4. At the 14th day, a significantly higher percentage of re-epithelization occurred only in the PVA/CHI/Gent treated group compared to the Ctr group ($p<0.05$) (Figure 4 A, B, C, D). Crust formation was observed in all experimental groups (Figure 4 A, B, C), with no significant differences in the thickness of the newly formed epithelium. In the Ctr group, some animals exhibited all epidermal strata, while others showed only the *stratum germinativum*, or both the *stratum germinativum* and *stratum granulosum*. This pattern was also seen in the PVA/Gent group, however, animals in the PVA/CHI/Gent group showed the presence of all stratums in the newly formed epidermis. During the 21st day period the higher percentage of re-epithelization was significant in the PVA/Gent treated groups compared to the Ctr group ($p<0.05$) (Figure 4 E, F, G, H). The crust was present solely in the Ctr group (Figure 4 E), and as in previous periods, there were no significant differences in the thickness of the newly formed epithelium among the experimental groups. By the 21st day, every animal in each group exhibited all stratums in the newly formed epidermis.

 doi:10.20944/preprints202504.0504.v1

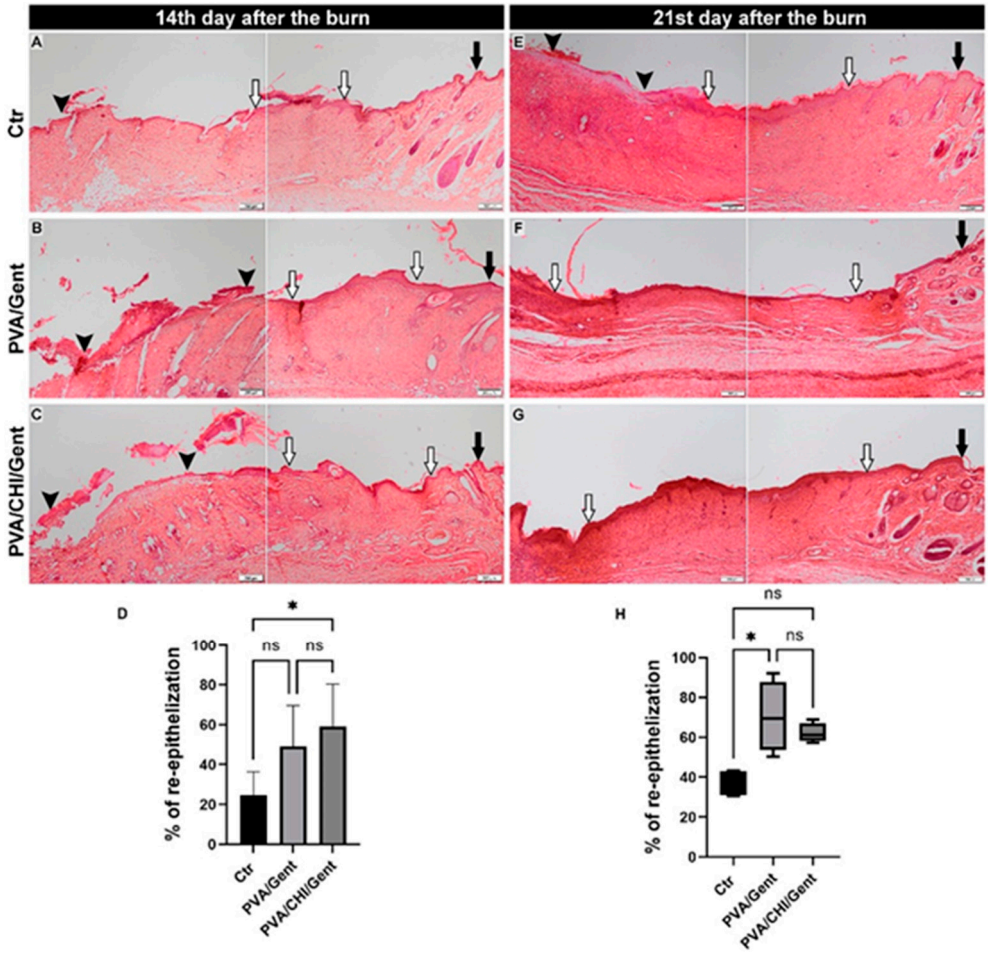

Figure 4. Representative photomicrographs of the burn wounds from the (**A, E**) Ctr group; (**B, F**) PVA/Gent treated group; (**C, G**) PVA/CHI/Gent treated group (**black arrow** – intact skin; **white arrow** – newly formed epithelium; **black arrowhead** – crust); (**A - G**) Tissue sections stained with hematoxylin/eosin and viewed with a scanning (4x), objective (bar: 200 μm); (**D**) Bar graph showcasing the percentage of re-epithelization at the 14th day period compared by the one-way ANOVA + Tukey test with data presented as mean ± standard deviation; (**H**) Boxplot showcasing the percentage of re-epithelization at the 21st day period compared by Kruskal-Wallis test + Dunn's test. Boxes indicate the lower to upper quartile (25th-75th percentile) and median value. Whiskers extend to minimum and maximum values. Statistical significance is denoted as * $p<0.05$.

Various studies examining the effectiveness of hydrogels containing different combinations of PVA, CHI and Gent with or without other polymers showed beneficial effect on the process of re-epithelization [15,40,41]. To the best of our knowledge this study is the first explaining the beneficial effects of the exact combination of PVA/Gent and PVA/CHI/Gent hydrogels. The enhanced re-epithelization could be explained by the fact that moist environment enables the faster migration of keratinocytes [42]. The effects were evident earlier in the PVA/CHI/Gent treated group which can be explained by the synergy between the moist environment and CHI activating various cells (neutrophils, macrophages and fibroblasts) to produce cytokines which enables optimal condition for keratinocytes migration [43].

The individual scores for all parameters assessed in the dermis of the burn wound (subepithelial neutrophils, fibroblasts, collagen deposition, edema and angiogenesis) are graphically represented in heat maps in Figure 5, while the representative photomicrographs of the assessments are presented in Figure 6.

 doi:10.20944/preprints202504.0504.v1

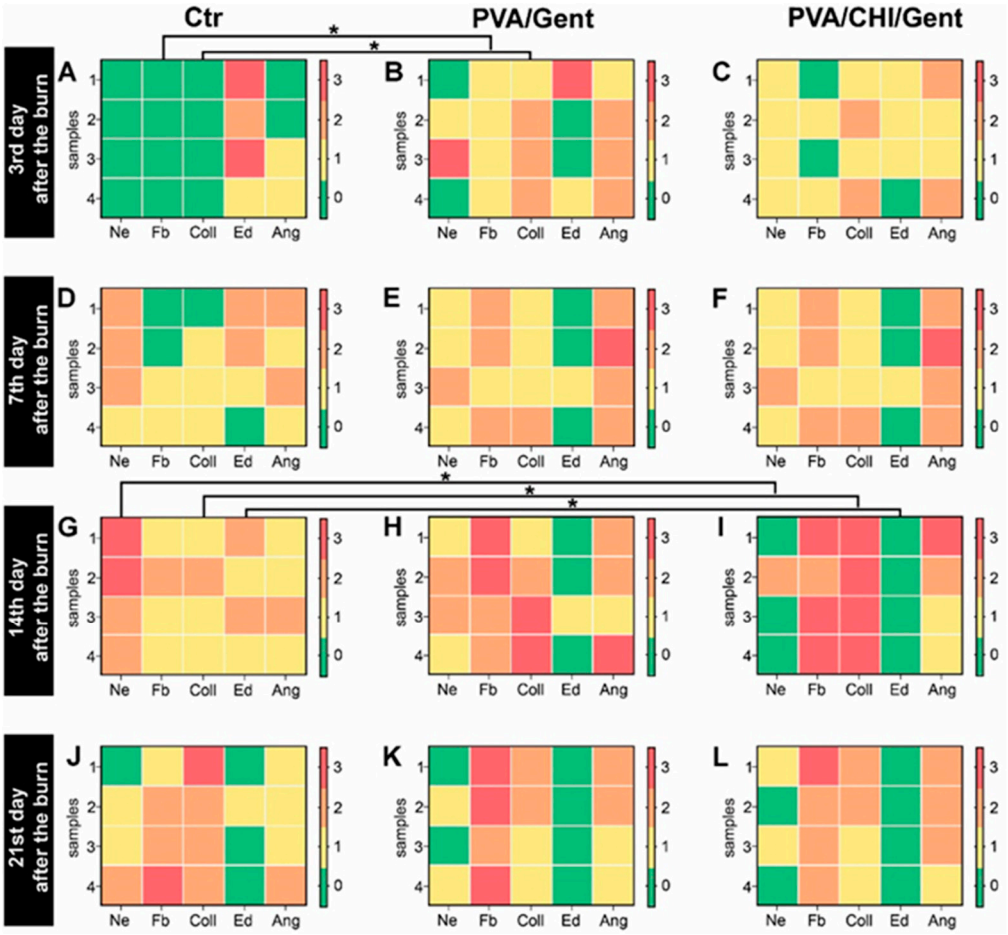

Figure 5. Heat maps showcasing the scores for all parameters [subepithelial neutrophils (Ne), fibroblasts (Fb), collagen deposition (Coll), edema (Ed) and angiogenesis (Ang)] assessed in the dermis of the burn wounds at 3rd, 7th, 14th and 21st day periods in the Ctr, PVA/Gent and PVA/CHI/Gent treated groups. The lines of significance are drawn between the columns representing the parameters that are significantly different between experimental groups. Statistical significance is denoted as * $p<0.05$.

 doi:10.20944/preprints202504.0504.v1

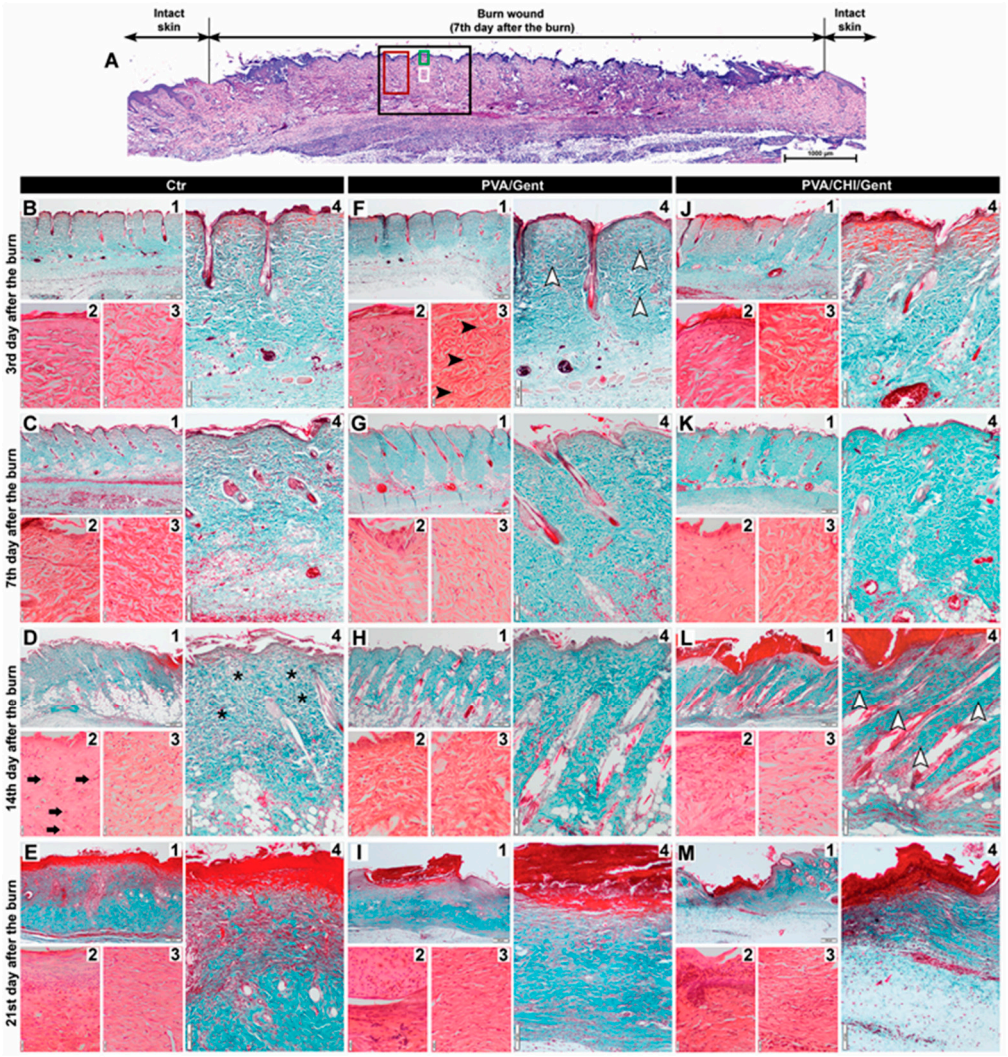

Figure 6. Photomicrographs of the burn wounds showcasing the parameters assessed in the dermis. (**A**) Composed photomicrograph illustrating the regions of the burn wound shown in other photomicrographs in this figure (**black rectangle** – region shown in photomicrographs 1; **green rectangle** – region shown in photomicrographs 2; **white rectangle** – region shown in photomicrographs 3; **red rectangle** – region shown in photomicrograph 4); (**B1 - B4, C1 - C4, D1 - D4, E1 - E4**) Burn wound sections of the Ctr; (**F1 - F4, G1 - G4, H1 - H4, I1 - I4**) PVA/Gent treated group; (**J1 - J4, K1 - K4, L1 - L4, M1 - M4**) PVA/CHI/Gent treated group (**black arrowhead** – fibroblasts; **white arrowhead** - collagen fibers; **black arrow** - subepithelial neutrophils; **black star** – edema). The parameters are marked in photomicrographs of groups in which there was a significant difference in scores of that parameter compared to other groups. Burn wound sections stained with Masson Goldner (**B1 - M1**) viewed with a scanning (4x) objective, (bar: 200 μm) and (**B4 - M4)** low power (x10) objective, (bar: 100 μm). Burn wound sections stained with Hematoxylin/Eosin (**B2, B3 - M2, M3**) viewed with a high power (x40) objective, (bar: 20 μm).

At the 3rd day period, all parameters in the treated groups showed higher grades, except for edema, which was rated higher in the Ctr group (Figure 5 A, B, C). Significant differences were noted for fibroblast count and collagen deposition, with the PVA/Gent treated group showing notably higher levels compared to the Ctr group ($p<0.05$) (Figure 5 A, B, C and Figure 6 B3, B4, F3, F4). These findings suggest that the PVA/Gent hydrogel positively influences early wound healing by enhancing fibroblast proliferation and collagen synthesis. This observation aligns with *in vitro* studies where PVA hydrogels, even without added growth factors, induced slight increases in fibroblast proliferation and facilitated transit of cells [44]. The more pronounced increase in fibroblasts observed in our study may be attributed to the *in vivo* setting and the presence of different cells, namely neutrophils during the inflammatory phase. Neutrophils protect the wound from infection and clear

 doi:10.20944/preprints202504.0504.v1

tissue debris [45], while also stimulating fibroblast proliferation both directly, via cytokine expression (IL-8, IL-1β, MCP-1), and indirectly by attracting macrophages, which further enhance fibroblast activity [46]. The significant increase in collagen deposition in the PVA/Gent group on the 3rd day is likely a direct consequence of the elevated fibroblast presence, considering the fact that the collagen is mostly synthesized by fibroblasts [45].

By the 7th day, edema remained more prominent in the Ctr group, which also exhibited higher grades of subepithelial neutrophils (Figure 5 D, E, F). Although fibroblast count, collagen deposition, and angiogenesis continued to be more pronounced in the treated groups, no significant differences were observed at this time point. This lack of significance may reflect the transitional phase of wound healing, where the inflammatory response begins to subside, and proliferative processes take precedence.

The trend persisted into the 14th day period, where the Ctr group had higher grades of subepithelial neutrophils and edema, with significant reductions in these parameters in the PVA/CHI/Gent group ($p<0.05$) (Figure 5 G, H, I and Figure 6 D2, D4, L2, L4). Fibroblast count, collagen deposition, and angiogenesis remained more pronounced in the treated groups, with collagen deposition significantly higher in the PVA/CHI/Gent group ($p<0.05$) (Figure 5 H, I, J and Figure 6 D4, L4). The delayed, but significant effects of the PVA/CHI/Gent hydrogel likely result from the synergistic antimicrobial action of CHI and Gent. Chitosan's antimicrobial activity, based on its positive charge interacting with negatively charged bacterial cell membranes, enhances permeability, while Gent's limited cell penetration is overcome by CHI's effect [47,48]. Reduced subepithelial neutrophil presence and edema in the PVA/CHI/Gent group may thus reflect decreased inflammation due to the combined antibacterial action, which is consistent with our antibacterial activity tests and supported by literature [49]. Such enhanced antibacterial effects are desirable in wound dressings to prevent biofilm formation and bacterial adhesion during the critical early stages of healing. Also, the time-dependent release of the antibacterial agent would ensure prolonged sterility of the dressing and the wound itself. Moreover, the significant increase in collagen deposition at 14th day period in the PVA/CHI/Gent group aligns with previous findings where CHI stimulated collagen synthesis by enhancing prolyl hydroxylase activity in granulation tissue [50]. This enzyme's peak activity at the 14th post-implantation day matches the elevated collagen levels observed in our study, reinforcing the efficacy of the PVA/CHI/Gent hydrogel in supporting the proliferative phase of wound healing.

By the 21st day, edema was no longer visible in any observed group (Figure 5 J, K, L and Figure 6 E4, I4, M4). Although the Ctr group still exhibited more subepithelial neutrophils in the dermis, collagen deposition was rated higher in this group for the first time (Figure 5 J, K, L). Fibroblast presence and angiogenesis consistently remained higher in the treated groups, though none of the differences during this period reached significance. These results suggest that while initial inflammation is mitigated by the hydrogel treatments, long-term matrix remodeling processes like collagen deposition may vary depending on the wound environment and treatment dynamics.

3. Conclusions

The novel PVA/Gent and PVA/CHI/Gent hydrogels demonstrated significant wound healing efficacy in second-degree burn wounds. The hydrogels showed good handling and hydrophilicity adhering well to the wound bed. Both hydrogels had significantly reduced inflammation and exhibited strong antibacterial properties. They enhanced re-epithelization and increased fibroblast proliferation and collagen deposition in the healing process. Both PVA/Gent and PVA/CHI/Gent hydrogels show potential as effective wound dressings, promoting faster healing and improved tissue recovery.

4. Materials and Methods

4.1. Materials

 doi:10.20944/preprints202504.0504.v1

The following chemicals were utilized for preparation of PVA/Gent and PVA/CHI/Gent hydrogels: poly(vinyl alcohol) powder (fully hydrolyzed, Mw = 70-100 kDa, Sigma Aldrich, USA), chitosan powder (Mw = 190-310 kDa, deacetylation degree 75-85 %, Sigma Aldrich, USA) and gentamicin sulfate solution (50 mg/ml in dH_2O, Sigma Aldrich, USA). Deionized water was obtained by passing the distilled water through a GenPure ultrapure water system (TKA, Germany).

4.1.1. Synthesis of PVA/Gent Hydrogel

Colloid dispersion of PVA (10 wt.%) was prepared by dissolving PVA powder in hot distilled water at 90ºC for 2h, under magnetic stirring. The PVA hydrogels were obtained by physical cross linking of PVA dispersion using freezing-thawing method in 5 cycles. One cycle consisted of freezing for 16h at -18ºC, followed by thawing for 8h at 4ºC. Thus, obtained hydrogels were cut into discs with diameters, d, of 10 mm and thicknesses, δ, of 4 mm. Then, the hydrogels were swollen in 5.0 mg/ml gentamicin solution at 37ºC during 48h, to obtain PVA/Gent hydrogels.

4.1.2. Synthesis of PVA/CHI/Gent Hydrogel

Colloid dispersion of PVA was prepared by dissolving PVA powder in hot distilled water at 90ºC for 2h, under magnetic stirring. Chitosan was dissolved in 2 vol% CH_3COOH under constant stirring at room temperature. After cooling of PVA, the CHI dispersion was added dropwise and the final dispersions (containing 10 wt.% PVA and 0.5 wt.% CHI) were homogenized by mixing at room temperature for 2-3h. Further, the PVA/CHI hydrogels were prepared by physical cross linking of PVA/CHI dispersion using freezing-thawing method in 5 cycles. One cycle consisted of 16h freezing at -18°C followed by 8h thawing at 4°C. Finally, the hydrogels were swollen in 5.0 mg/ml gentamicin solution at 37ºC during 48h, to obtain PVA/CHI/Gent hydrogels.

4.1.3. Antibacterial Activity

Antibacterial activity of PVA/Gent and PVA/CHI/Gent hydrogels was investigated against Gram-negative and Gram-positive bacteria strains – *Escherichia coli* ATCC 25922 and *Staphylococcus aureus* TL (culture collection Faculty of Technology and Metallurgy, University of Belgrade, Serbia). Hydrogels were sterilized in the laminar air flow chamber by exposure to a UV-C lamp (30 min, 60 cm lamp distance) and their antibacterial activity was evaluated by disc-diffusion method. A soft-top agar (0.7 wt.%, 15 ml) was melted, cooled down to ~55°C and inoculated with bacteria cultures (150 µl) overnight (~18h), then gently stirred and poured over previously solidified nutrient agar base in sterile Petri dishes. Number of bacteria in the nutrient soft-top agar layer was set to be ~10^6 CFU ml^{-1}. After solidification of soft-top agar, hydrogel disc samples were placed on its surface. The inhibition zone widths were measured after 24h incubation at 37°C.

4.1.4. Gentamicin Release

High-performance liquid chromatography (HPLC) (Thermo Fisher Scientific, USA) was utilized for Gent components separation and the detection and quantitative analysis were done in an ion trap mass spectrometer (MS) (LCQ Advantage, Thermo Fisher Scientific). High-performance liquid chromatography was equipped with a reverse-phase column (4.6 mm × 75 mm × 3.5 µm) Zorbax Eclipse® XDB-C18 (Agilent Technologies, USA), in front of which a precolumn (4.6 mm × 12.5 mm × 5 µm) was placed. Methanol (A), deionized water (B), and 10% acetic acid (C) comprised the mobile phase. The optimized HPLC and MS operating parameters (mobile-phase gradient, analytes' precursor ions, fragmentation reactions used for quantification, and optimal collision energies) for the determination of Gent compounds were published in our previous paper [51]. The gentamicin mass spectra were collected in the m/z range of 50-1000. As expected, the MS spectrum revealed the three most abundant ions since Gent is composed of three compounds – Gent C1a, C2, and C1. These ions were further chosen as the precursor ions for each compound. Their most sensitive transitions

 doi:10.20944/preprints202504.0504.v1

were selected for quantification purposes. The presented Gent concentrations represent sums of the three determined Gent compounds.

4.2. Animals

Three-month-old male Wistar rats weighing 300-330g obtained from the Department of Laboratory and Experimental Care and Use of Animals Unit of the Institute of Medical Research, Military Medical Academy (Belgrade, Serbia) were used in the experiment. Rats were housed individually in polypropylene cages in an air-conditioned animal facility, under standard conditions with a photoperiodic cycle of 12h light: 12h darkness, and food and water intake *ad libitum*. All of the experimental procedures were approved by the Ethical Committee of the Faculty of Veterinary Medicine University of Belgrade and by the Ministry of agriculture, forestry and water management – veterinary administration (decision number 323-07-04903/2022-05/1). The experiment and animal handling were carried out in accordance with the ARRIVE guidelines and the European Union's Directive 2010/63/EU on the Protection of Animals Used for Scientific Purposes.

4.2.1. Experimental Design

Burn wounds were modeled following the protocol by Tavares Pereira et al. [30]. The procedure utilized general anesthesia with intraperitoneal injections of 75 mg/kg ketamine hydrochloride (Ketamidor 10%, 100mg/ml, RICHTER PHARMA AG, Austria) and 10 mg/kg xylazine (Xylased 2%, BIOVETA, Czech Republic). After trichotomy of the back skin and disinfection with povidone-iodine, a thermal injury was induced by applying a solid aluminum bar (10 mm diameter, mass of 51g), previously heated in boiling water (temperature of 100°C), to the skin of the dorsal proximal region for 15 seconds without any additional pressure. Post-procedure, animals received intramuscular analgesia with 5 mg/kg Ketoprofen (Ketonal, á 100mg/2ml, SANDOZ, Switzerland), for three consecutive days.

Following the burns, animals were randomly assigned to three experimental groups: control (Ctr) (n=16), PVA/Gent treated (n=16), and PVA/CHI/Gent treated group (n=16), with daily dressing of the wounds. Clinical evaluations of the burn wounds were conducted on the 3rd, 7th, 14th, and 21st day by semi-quantitatively assessing the parameters such as blistering, edema, redness, crust, bleeding, secretion, and scar tissue, on a scale from 0 (absent) to 3 (severe). Diameters of the burn were measured immediately after burn induction and on previously specified days to calculate wound contraction using the Eqs. (6):

$$X_{\%} = [X_0 - X/X_0] * 100 \quad (2)$$

Here, $X_{\%}$ is percentage of wound contraction on the specified day, X_0 is the initial diameter of the wound and X is diameter of the wound on the specified day. On those evaluation days, four animals from each group were euthanized using 100 mg/kg Euthasol Euthanasia Solution (Produlab Pharma Production B.V., Raamsdonksveer, Netherlands) for histological sample collection.

4.2.2. Histological Analysis

During sampling, a square piece of skin containing the entire burn wound was taken and bisected along the diameter of the circular burn. Both halves of each sample were fixed and processed by conventional manner for histological examination. Paraffin-embedded tissue blocks were serially sectioned and stained with Hematoxylin-Eosin (H/E) and Masson Goldner (MG) staining kit (Merck Millipore, Darmstadt, Germany), then evaluated on a standard Olympus CX31 microscope equipped with a digital camera and software (UC50 Soft Imaging Solutions camera and SensEntry 1.13 software, Münster, Germany). Histological analyses included the assessments of re-epithelization at the 14th and 21st day and evaluations of the dermis at all time points.

Re-epithelization process was evaluated on H/E stained sections at 4x magnification by calculating the percentage of re-epithelization $X_{e\%}$ on the specified day using the formula: $X_{e\%} = (X_e/X_e + X) * 100$, where X_e is the length of newly formed epithelium on the specified day and X is

 doi:10.20944/preprints202504.0504.v1

the length of open wound on the specified day. Additionally, the thickness of the newly formed epithelium was measured at five points; approximately 300 μm from the wound edges on both sides of the burn wound, at 40x magnification and the stratification in the epithelium was assessed.

The semi-quantitative assessment of the dermis evaluated the percentage of dermal coverage by subepithelial neutrophils, fibroblasts, collagen deposition, edema, and angiogenesis at 40x magnification. Each parameter was scored as absent (0) for up to 10%, mild (1) for 10-40%, moderate (2) for 40-70%, and severe (3) for 70-100% coverage. All parameters were assessed on H/E stained sections, except collagen deposition, which was estimated on MG stained sections.

4.3. Statistical Analysis

All collected data were analyzed in the GraphPad Prism 9 software (GraphPad, San Diego, CA, USA). Prior to the applying of the statistical analysis the normality of data distribution was tested using the Shapiro-Wilk normality test. All histological examination results were analyzed using the Kruskal-Wallis test followed by Dunn's post-hoc test, except for the re-epithelization assessment on day 14th, which was analyzed using one-way ANOVA followed by Tukey's post-hoc test.

Author Contributions: Conceptualization, V.M.S. and D.M.; Methodology, T.L.B., A.J., B.B.P., I.M. and A.N.; Validation, A.J., I.M., T.L.B. and M.V.S.; Formal analysis, A.N. and M.S.; X.X.; Investigation, A.J., M.S., B.B.P., I.M., E.N., A.N. and T.L.B.; Resources, V.M.S., A.J., D.M. and T.L.B.; Writing—original draft preparation, A.J., M.V.S., T.L.B. and A.N.; Writing—review and editing, V.M.S., D.M., I.M. and B.B.P.; Visualization, I.M. and A.J.; Supervision, A.J., V.M.S., D.M. and T.L.B. All authors have read and agreed to the published version of the manuscript.

Funding: The study was supported by the Ministry of Science, Technological Development and Innovation of the Republic of Serbia (Contracts number: 451-03-136/2025-03/200143, 451-03-136/2025-03/200287, 451-03-136/2025-03/200135 and 337-00-110/2023-05/13)**.**

Institutional Review Board Statement: The animal study protocol was approved by the Ethical Committee of the Faculty of Veterinary Medicine University of Belgrade and by the Ministry of agriculture, forestry and water management – veterinary administration (Decision number 323-07-04903/2022-05/1)

Data Availability Statement: The data that support the findings of this study are available from the corresponding author upon reasonable request.

Acknowledgments: The authors extend their special thanks to Aleksandra Todić, the Laboratory Technician in the Department of Histology and Embryology at the Faculty of Veterinary Medicine, University of Belgrade, for her expert support throughout all stages of this study, including animal care, tissue sampling and processing, as well as histological sample preparation.

Conflicts of Interest: The authors declare no conflicts of interest.

References

1. Baglio, S.R.; Pegtel, D.M.; Baldini, N. Mesenchymal stem cell secreted vesicles provide novel opportunities in (stem) cell-free therapy. *Front. Physiol.* **2012**, *3*, 359. https://doi.org/10.3389/fphys.2012.00359.
2. Gantwerker, E.A.; Hom, D.B. Skin: histology and physiology of wound healing. *Clin. Plast. Surg.* **2012**, *39*, 85–97. https://doi.org/10.1016/j.cps.2011.09.005.
3. Zhang, X.; Shu, W.; Yu, Q.; Qu, W.; Wang, Y.; Li, R. Functional biomaterials for treatment of chronic wound. *Front. Bioeng. Biotech.* **2020**, *8*, 516. https://doi.org/10.3389/fbioe.2020.00516.
4. Das, S.; Baker, A.B. Biomaterials and nanotherapeutics for enhancing skin wound healing. *Front. Bioeng. Biotech.* **2016**, *4*, 82. https://doi.org/10.3389/fbioe.2016.00082.
5. Mickelson, M.A.; Mans, C.; Colopy, S.A. Principles of Wound Management and Wound Healing in Exotic Pets. *Ve.t Clin. North. Am. – Exot. Anim. Pract.* **2016**, *19*, 33-53. https://doi.org/10.1016/j.cvex.2015.08.002.
6. Ebhodaghe, S.O. Hydrogel–based biopolymers for regenerative medicine applications: a critical review. *Int. J. Polym. Mater.* **2022**, *71*, 155–172. https://doi.org/10.1080/00914037.2020.1809409.

 doi:10.20944/preprints202504.0504.v1

7. Aderibigbe, B.; Buyana, B. Alginate in wound dressings. *Pharmaceutics* **2018**, *10*, 42. https://doi.org/10.3390/pharmaceutics10020042.
8. Ahsan, A.; Tian, W.X.; Farooq, M.A.; Khan, D.H. An overview of hydrogels and their role in transdermal drug delivery. *Int. J. Polym. Mater.* **2021**, *70*, 574–584. https://doi.org/10.1080/00914037.2020.1740989.
9. Shanshan, J.; Newton, M.A.A.; Cheng, H.; Zhang, Q.; Gao, W.; Zheng, Y.; Lu, Z.; Dai, Z.; Zhu, J. Progress of Hydrogel Dressings with Wound Monitoring and Treatment Functions. *Gels* **2023**, *9*, 694. https://doi.org/10.3390/gels9090694.
10. Suflet, D.M.; Popescu, I.; Pelin, I.M.; Ichim, D.L.; Daraba, O.M.; Constantin, M.; Fundueanu, G. Dual cross-linked chitosan/PVA hydrogels containing silver nanoparticles with antimicrobial properties. *Pharmaceutics* **2021**, *13*, 1461. https://doi.org/10.3390/pharmaceutics13091461.
11. Lužajić Božinovski, T.; Todorović, V.; Milošević, I.; Prokić, B.B.; Gajdov, V.; Nešović, K.; Mišković-Stanković, V.; Marković, D. Macrophages, the main marker in biocompatibility evaluation of new hydrogels after subcutaneous implantation in rats. *J. Biomater. Appl.* **2022**, *36*, 1111–1125. https://doi.org/10.1177/08853282211046119.
12. Shamloo, A.; Aghababaie, Z.; Afjoul, H.; Jami, M.; Bidgoli, M.R.; Vossoughi, M.; Ramazani, A.; Kamyabhesari, K. Fabrication and evaluation of chitosan/gelatin/PVA hydrogel incorporating honey for wound healing applications: An in vitro, in vivo study. *Int. J. Pharmaceut.* **2021**, *592*, 120068. https://doi.org/10.1016/j.ijpharm.2020.120068.
13. Alavi, M.; Nokhodchi, A. An overview on antimicrobial and wound healing properties of ZnO nanobiofilms, hydrogels, and bionanocomposites based on cellulose, chitosan, and alginate polymers. *Carbohyd. Polym.* **2020**, *227*, 115349. https://doi.org/10.1016/j.carbpol.2019.115349.
14. Stoica, A.E.; Chircov, C.; Grumezescu, A.M. Nanomaterials for Wound Dressings: An Up-to-Date Overview. *Molecules* **2020**, *25*, 2699. https://doi.org/10.3390/molecules25112699.
15. Yan, T.; Kong, S.; Ouyang, Q.; Li, C.; Hou, T.; Chen, Y.; Li, S. Chitosan-Gentamicin Conjugate Hydrogel Promoting Skin Scald Repair. *Mar. Drugs* **2020**, *18*, 233. https://doi.org/10.3390/md18050233.
16. Iannuccelli, V.; Maretti, E.; Bellini, A.; Malferrari, D.; Ori, G.; Montorsi, M.; Bondi, M.; Truzzi, E.; Leo, E. Organo-modified bentonite for gentamicin topical application: Interlayer structure and in vivo skin permeation. *Appl. Clay Sci.* **2018**, *158*, 158–168. https://doi.org/10.1016/j.clay.2018.03.029.
17. No, H.K.; Park, N.Y.; Lee, S.H.; Meyers, S.P. Antibacterial activity of chitosans and chitosanoligomers with different molecular weights. *Int. J. Food Microbiol.* **2002**, *74*, 65–72. https://doi.org/10.1016/S0168-1605(01)00717-6.
18. Balakumar, P.; Rohilla, A.; Thangathirupathi, A. Gentamicin-induced nephrotoxicity: Do we have a promising therapeutic approach to blunt it?. *Pharmacol. Res.* **2010**, *62*, 179–186. https://doi.org/10.1016/j.phrs.2010.04.004.
19. Forge, A.; Schacht, J. Aminoglycoside antibiotics. *Audiol. Neurotol.* **2000**, *5*, 3–22. https://doi.org/10.1159/000013861.
20. Monteiro, N.; Martins, M.; Martins, A.; Fonseca, N.A.; Moreira, J.N.; Reis, R.L.; Neves, N.M. Antibacterial activity of chitosan nanofiber meshes with liposomes immobilized releasing gentamicin. *Acta Biomater.* **2015**, *18*, 196–205. https://doi.org/10.1016/j.actbio.2015.02.018.
21. Zalavras, C.G.; Patzakis, M.J.; Holtom, P.; Local Antibiotic Therapy in the Treatment of Open Fractures and Osteomyelitis. *Clin. Orthop. Relat. R.* **2004**, *427*, 86–93. https://doi.org/10.1097/01.blo.0000143571.18892.8d.
22. Mišković-Stanković, V.; Janković, A.; Grujić, S.; Matić-Bujagić, I.; Radojević, V.; Vukašinović-Sekulić, M.; Kojić, V.; Djošić, M.; Atanacković, T.M. Diffusion models of gentamicin released in poly(vinyl alcohol)/chitosan hydrogel. *J. Serb. Chem. Soc.* **2024**, *89*, 627–641. https://doi.org/10.2298/JSC231207010M.
23. Yoshizawa S. Structural origins of gentamicin antibiotic action. *EMBO J* **1998**, *17*, 6437-48. https://doi.org/10.1093/emboj/17.22.6437.
24. Makoid, M. C.; Dufour, A.; Banakar U. V. Modelling of Dissolution Behaviour of Controlled Release Systems. *S.T.P. Pharma Pratiques* **1993**, *3*, 49–58.
25. Korsmeyer, R.W.; Gurny, R.; Doelker, E.; Buri, P.; Peppas, N.A. Mechanisms of Solute Release from Porous Hydrophilic Polymers. *Int. J. Pharmaceut.* **1983**, *15*, 25–35. https://doi.org/10.1016/0378-5173(83)90064-9.

 doi:10.20944/preprints202504.0504.v1

26. Kopcha, M.; Lordi, N.G.; Tojo, K.J. Evaluation of Release from Selected Thermosoftening Vehicles. *J. Pharm. Pharmacol.* **1991**, *43*, 382–87. https://doi.org/10.1111/j.2042-7158.1991.tb03493.x.ž.
27. Ritger, P.L.; Peppas, N.A. A Simple Equation for Description of Solute Release I. Fickian and Non-Fickian Release from Non-Swellable Devices in the Form of Slabs, Spheres, Cylinders or Discs. *J. Control. Release* **1987**, *5*, 23–36. https://doi.org/10.1016/0168-3659(87)90034-4.
28. Mišković-Stanković, V.; Atanackovic, T. *Novel antibacterial biomaterials for medical applications and modeling of drug release process*, 1st ed.; Taylor & Francis/CRC Press: Boca Raton, USA, 2024; pp.1-288. https://www.routledge.com/Novel-Antibacterial-Biomaterials-for-Medical-Applications-and-Modeling-of-Drug-Release-Process/Miskovic-Stankovic-Atanackovic/p/book/9781032668864.
29. Sjögren, G.; Sletten, G.; Dahl, E.J. Cytotoxicity of dental alloys, metals, and ceramics assessed by Millipore filter, agar overlay, and MTT tests. *J. Prosthet. Dent.* **2000**, *84*, 229–236. https://doi.org/10.1067/mpr.2000.107227.
30. Tavares Pereira, D.D.S.; Lima-Ribeiro, M.H.M.; de Pontes-Filho, N.T.; Carneiro-Leão, A.M.D.A.; Correia, M.T.D.S. Development of animal model for studying deep second-degree thermal burns. *BioMed Res. Int.* **2012**, *1*, 460841. https://doi.org/10.1155/2012/460841.
31. Stojkovska, J.; Djurdjevic, Z.; Jancic, I.; Bufan, B.; Milenkovic, M.; Jankovic, R.; Mišković-Stanković, V.; Obradovic, B. Comparative in vivo evaluation of novel formulations based on alginate and silver nanoparticles for wound treatments. *J. Biomater. Appl.* **2018**, *32*, 1197–1211. https://doi.org/10.1177/0885328218759564.
32. Firat, C.; Samdanci, E.; Erbatur, S.; Aytekin, A.H.; Ak, M.; Turtay, M.G.; Coban, Y.K. β-Glucan treatment prevents progressive burn ischaemia in the zone of stasis and improves burn healing: an experimental study in rats. *Burns* **2013**, *39*, 105–112. https://doi.org/10.1016/j.burns.2012.02.031.
33. Gal, P.; Kilik, R.; Mokry, M.; Vidinsky, B.; Vasilenko, T.; Mozes, S.; Bobrov, N.; Tomori, Z.; Bober, J.; Lenhardt, L. Simple method of open skin wound healing model in corticosteroid-treated and diabetic rats: standardization of semi-quantitative and quantitative histological assessments. *Vet. Med-Czech* **2008**, *53*, 652–659. http://dx.doi.org/10.17221/1973-VETMED.
34. Nunes, P.S.; Albuquerque Jr, R.L.; Cavalcante, D.R.; Dantas, M.D.M.; Cardoso, J.C.; Bezerra, M.S.; Souza, J.C.C.; Serafini, M.R.; Quitans, L.J.; Bonjardim Jr, L.R.; Araújo, A.A.S. Collagen-based films containing liposome-loaded usnic acid as dressing for dermal burn healing. *J. Biomed. Biotechnol.* **2011**, *2011*, 1–9. https://doi.org/10.1155/2011/761593.
35. Sabol, F.; Dancakova, L.; Gal, P.; Vasilenko, T.; Novotny, M.; Smetana, K.; Lenhardt, L. Immunohistological changes in skin wounds during the early periods of healing in a rat model. *Vet. Med-Czech* **2012**, *57*, 77–82. http://dx.doi.org/10.17221/5253-VETMED.
36. Tedgui, A. Focus on inflammation. *Arterioscler. Thromb. Vasc. Biol.* **2011**, *31*, 958–959. https://doi.org/10.1161/atvbaha.111.227355.
37. Cheung, R.C.F.; Ng, T.B.; Wong, J.H.; Chan, W.Y. Chitosan: An update on potential biomedical and pharmaceutical applications. *Mar. Drugs* **2015**, *13*, 5156-5186. https://doi.org/10.3390/md13085156.
38. Wang, T.; Zhu, X.K.; Xue, X.T.; Wu, D.Y. Hydrogel sheets of chitosan, honey and gelatin as burn wound dressings. *Carbohyd. Polym.* **2012**, *88*, 75-83. https://doi.org/10.1016/j.carbpol.2011.11.069.
39. Jin, Y.; Ling, P.X.; He, Y.L.; Zhang, T.M. Effects of chitosan and heparin on early extension of burns. *Burns* **2007**, *33*, 1027–1031. https://doi.org/10.1016/j.burns.2006.12.002.
40. Bakhsheshi-Rad, H.R.; Hadisi, Z.; Ismail, A.F.; Aziz, M.; Akbari, M.; Berto, F.; Chen, X.B. In vitro and in vivo evaluation of chitosan-alginate/gentamicin wound dressing nanofibrous with high antibacterial performance. *Polym. Test.* **2020**, *82*, 106298. https://doi.org/10.1016/j.polymertesting.2019.106298.
41. Hwang, M.R.; Kim, J.O.; Lee, J.H.; Kim, Y.I.; Kim, J.H.; Chang, S.W.; Jin, S.G.; Kim, J.A.; Lyoo, W.S.; Han, S.S.; Ku, S.K.; Yong, C.S.; Choi, H.G. Gentamicin-loaded wound dressing with polyvinyl alcohol/dextran hydrogel: gel characterization and in vivo healing evaluation. *AAPS PharmSciTech* **2010**, *11*, 1092–1103. https://doi.org/10.1208/s12249-010-9474-0.
42. Winter, G.D.; Scales, J.T. Effect of air drying and dressings on the surface of a wound. *Nature* **1963**, *197*, 91-92. https://doi.org/10.1038/197091b0.

 doi:10.20944/preprints202504.0504.v1

43. Khodja, A.N.; Mahlous, M.; Tahtat, D.; Benamer, S.; Youcef, S.L.; Chader, H.; Mouhoub, L.; Sedgelmaci, M.; Ammi, N.; Mansouri, M.B.; Mameri, S. Evaluation of healing activity of PVA/chitosan hydrogels on deep second degree burn: pharmacological and toxicological tests. *Burns* **2013**, *39*, 98–104. https://doi.org/10.1016/j.burns.2012.05.021.
44. Sankari, L.; Fernandes, B.; Rebelatto, C.; Brofman, P. Evaluation of PVA hydrogel as an extracellular matrix for in vitro study of fibroblast proliferation. *Int. J. Polym. Mater.* **2019**, *69*, 653–658. https://doi.org/10.1080/00914037.2019.1596915.
45. Diller, R.B.; Tabor, A.J. The Role of the Extracellular Matrix (ECM) in Wound Healing: A Review. *Biomimetics* **2022**, *7*, 87. https://doi.org/10.3390/biomimetics7030087.
46. Ellis, S.; Lin, E.J.; Tartar, D. Immunology of Wound Healing. *Curr. Dermatol. Rep.* **2018**, *7*, 350–358. https://doi.org/10.1007/s13671-018-0234-9.
47. Dai, T.; Tanaka, M.; Huang, Y.Y.; Hamblin, M.R.; Chitosan preparations for wounds and burns: antimicrobial and wound-healing effects. *Expert Rev. Anti-Infe.* **2011**, *9*, 857–879. https://doi.org/10.1586/eri.11.59.
48. Bārzdiņa, A.; Plotniece, A.; Sobolev, A.; Pajuste, K.; Bandere, D.; Brangule, A. From Polymeric Nanoformulations to Polyphenols—Strategies for Enhancing the Efficacy and Drug Delivery of Gentamicin. *Antibiotics* **2024**, *13*, 305. https://doi.org/10.3390/antibiotics13040305.
49. Potara, M.; Jakab, E.; Damert, A.; Popescu, O.; Canpean, V.; Astilean, S. Synergistic antibacterial activity of chitosan-silver nanocomposites on Staphylococcus aureus. *Nanotechnology* **2011**, *22*, 135101. https://doi.org/10.1088/0957-4484/22/13/135101.
50. Kojima, K.; Okamoto, Y.; Kojima, K.; Miyatake, K.; Fujise, H.; Shigemasa, Y.; Minami, S. Effects of chitin and chitosan on collagen synthesis in wound healing. *J. Vet. Med. Sci.* **2004**, *66*, 1595–1598. https://doi.org/10.1292/jvms.66.1595.
51. Stevanović, M.; Djošić, M.; Janković, A.; Kojić, V.; Stojanović, J.; Grujić, S.; Matić Bujagić, I.; Rhee, K.Y.; Mišković-Stanković, V. The Chitosan-Based Bioactive Composite Coating on Titanium. *J. Mater. Res. Technol.* **2021**, *15*, 4461–74. https://doi.org/10.1016/j.jmrt.2021.10.072.